X-ray emission from a 650-fs laser-produced barium plasma

W. H. Goldstein
L-Division, Lawrence Livermore National Laboratory, P.O. Box 808, Livermore, California 94550

A. Zigler, P. G. Burkhalter, and D. J. Nagel
Naval Research Laboratory, Department of the Navy, Washington, DC 20375-5000

A. Bar-Shalom and J. Oreg
Nuclear Research Center of the Negev, Box 9001, Beer Sheva, Israel

T. S. Luk, A. McPherson, and C. K. Rhodes
University of Illinois at Chicago, Chicago, Illinois 60680
(Received 19 November 1992)

We have used x rays in the 9–15-Å band emitted from a solid target of BaF_2 irradiated by ~120 mJ of 248-nm radiation in a 650-fs full width at half maximum Gaussian laser pulse to characterize spectroscopically the resulting ultrashort-pulse laser-produced plasma. The emission was spectrally resolved but space and time integrated. By comparing the spectrum with unresolved-transition-array calculations and measurements of plasma emission from longer-pulse experiments, it is clear that ions as highly stripped as titaniumlike barium are present. We have successfully modeled the observed spectrum by assuming an optically thin source in local thermodynamic equilibrium (LTE) and using the supertransition-array theory [A. Bar-Shalom *et al.*, Phys. Rev. A **40**, 3183 (1989)] for emission from a hot, dense plasma. The model indicates that the emitting region is at comparatively low temperature (200–300 eV) and high electron density (10^{23}–10^{24} cm^{-3}). The degree of agreement between the model and the measured spectrum also suggests that the emitting plasma is near LTE. We conclude that the emission in this band arises from a solid-density plasma formed early in time, and is thus localized in both space and time. This interpretation is reinforced by LASNEX [G. B. Zimmerman and W. L. Kruer, Comments Plasma Phys. Controlled Fusion **11**, 51 (1975)] simulations that indicate that emission in this band closely tracks the laser pulse.

PACS number(s): 52.50.Jm, 32.30.Rj, 52.70.La

Ultrashort-pulse laser technology, providing subpicosecond pulse lengths and power densities of up to 10^{19} W/cm^2 from table-top systems, has significantly expanded the field of laser-produced plasma research. Applications presently under investigation include x-ray lasers [1], ultrashort-pulse x-ray flashlamps [2], and the study of the laser-matter interaction at high density and temperature [3]. Progress in these and other directions depends on understanding x-ray production in ultrashort-pulse laser-produced plasmas. Unfortunately, experimental investigations have generally been compromised by the lack of time- and space-resolved information. Broadband measurements have put the duration of the x-ray burst at less than 2 ps, for a 100-fs-long laser pulse [2], but, in general, time resolution has been sufficient only to put upper bounds on the duration of x-ray emission [4]. Pinhole cameras have yielded images of the emitting plasmas with resolutions down to about 5 μm [4,5], but this is insufficient to resolve a transient, solid-density plasma expected to extend over less than 500 nm, based on the absence of hydrodynamic motion and measurements of heat front penetration [6]. Prior attempts to characterize these plasmas based on spectroscopically resolved measurements have been limited to estimates of electron density using line broadening [4,7] in light elements. These analyses have encountered ambiguities owing to the long time scales involved in the atomic kinetics [4,7] and have involved short-pulse energy deposition in plasmas preformed by an amplified-spontaneous-emission (ASE) prepulse and consequently emitting at much lower than solid density [4,7,8].

In the absence of sufficient instrumental time and space resolution, it is important to explore spectral signatures that can be correlated with localized plasma conditions. Recently, Zigler *et al.* [5] measured intense x-ray emission from ultrashort-pulse laser-produced barium plasmas, formed without an ASE prepulse [9], at or near the maximum possible intensity. We have analyzed this spectrally resolved, but space- and time-integrated, emission in the 9–15-Å band created by 650-fs full width at half maximum (FWHM), 248-nm, KrF-laser pulses on solid targets of BaF_2. Time scales for the atomic kinetics of highly stripped barium should be short enough to remove atomic transients from the analysis. From the spectrum, we have been able to characterize the charge-state distribution, temperature, and density of the emitting plasma. For the latter two quantities, we have used the supertransition-array (STA) theory for heavy-element emission from plasma in local thermodynamic equilibrium (LTE) [10]. This method of spectral simulation is essential for

analyzing the quasicontinuum emission of many-electron systems at high density, in distinction to the simpler line spectra encountered in light-element plasmas even under ultrashort-pulse irradiation. Our conclusion is that this emission arises primarily from a cool, near-solid-density region, rather that from the hot, expanding corona, in contrast to the light-element emission seen in prepulse experiments [4,7,8]. This interpretation is supported by hydrodynamic simulations that further confirm that the emission is local in time.

The KrF laser for these experiments had a pulse width of 650 fs and an energy of 120 mJ, yielding a peak power of 200 GW and an average power density of $\sim 10^{17}$ W/cm^2. A 20-mJ prepulse was spread over ~ 20 ns. A detailed description of the laser system has been presented elsewhere [11]. The laser beam was focused onto a planar rotating target with a plano-convex $f/10$ CaF_2 lens. Several positions of the focusing lens were selected in order to vary the incident peak laser intensity. The x-ray emission from the target was collected by a flat potassium acid phthalate crystal ($2d = 26.6$ Å) spectrometers using Kodak DEF film. The calibration is described in Ref. [5]. Each spectrum was produced by 25 laser shots. Shot-to-shot variations in laser intensity were typically smaller than 10%, but could be as large as 50%. Ten shot averages always varied by less than 10%. The BaF_2 target was chosen since it is sufficiently transparent to low intensities of the uv laser that no prepulse plasma is formed [9]. Figure 1 shows the spectrum obtained with a laser intensity of 5×10^{15} W/cm^2. Figure 2 shows the spectrum, previously reported in Ref. [5], obtained at $\sim 10^{17}$ W/cm^2.

We turn now to analyzing the spectrum and plasma conditions. The lower trace in Fig. 1 shows an unresolved-transition-array (UTA) calculation [12] of the $3d$-$4f$ transitions in charge states of barium from scandiumlike through nickel-like. Comparing with this calculation, it is clear that the quasicontinuum emission in the

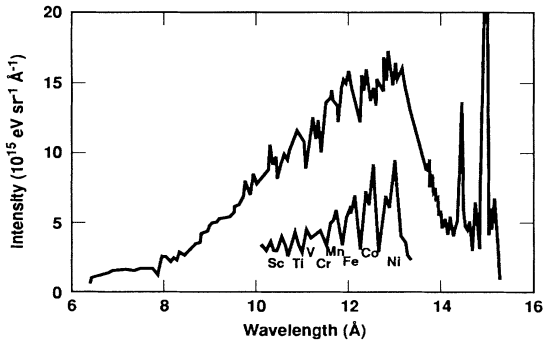

FIG. 1. Space- and time-integrated x-ray spectrum emitted by a barium plasma formed by ultrashort-pulse irradiation with 5×10^{15} W/cm^2 at $\lambda = 248$ nm. The vertical axis is intensity, in units of 5×10^{15} eV/sr Å. The narrow lines at long wavelength are fluorine He-β and H-α. The lower trace is a UTA calculation of the $3d$-$4f$ transition arrays in charge states of barium from scandiumlike through nickel-like. The calculated positions of these transition arrays indicates these same charge states contribute to the measured spectrum.

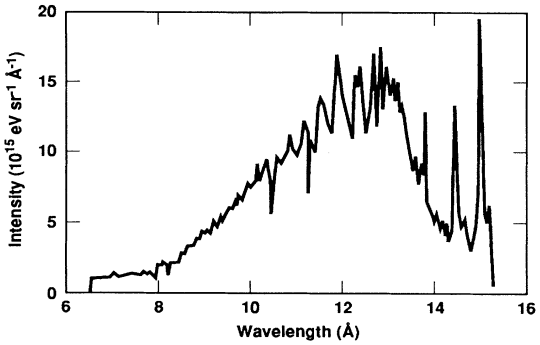

FIG. 2. Same as Fig. 1, but for an irradiation intensity of $\sim 10^{17}$ W/cm^2. (From Ref. [5].)

measured spectrum arises from the same charge states. If near-coronal conditions are obtained in the emitting plasma, this implies a fairly high temperature, on the order of 1 keV. On the other hand, if emission arises primarily from a near-solid-density plasma, conditions can be nearer LTE, and much lower temperatures are required. In fact, assuming Saha equilibrium, at solid density a temperature as low as 100 eV will strip barium beyond nickel-like. The almost complete absence of structure in the measured spectrum, as contrasted, for example, with the distinctive non-LTE, long pulse (4.5 ns) laser-produced plasma spectrum [13] in Fig. 3, supports the latter hypothesis, since, at high density, multistep collisional processes populate a huge array of states never sampled under non-LTE conditions, and these "satellites" fill in the spectrum. In Fig. 3, emission from specific charge states of barium have been identified using Cowan's atomic structure computer code [14].

We have modeled the barium spectrum shown in Fig. 1, assuming that it is emitted by an optically thin plasma in LTE. In Fig. 4(a), STA spectra are displayed for barium at normal density (3.5 g/cm^3) and a range of temperatures. The solid trace represents a weighted sum of the emission at the several temperatures shown. The weights were chosen to give a reasonably good fit to the data shown in Fig. 1. Though this is not a precise procedure, it conveys the essential point that the emission can be

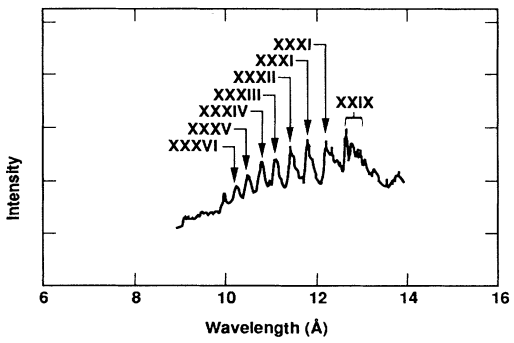

FIG. 3. Barium spectrum from a plasma formed by a 4.5 ns pulse. Contributing charge states between nickel-like Ba XXIX and scandiumlike Ba XXXVI are identified. Characteristically, the long-pulse laser-produced plasma is dominated by UTA's.

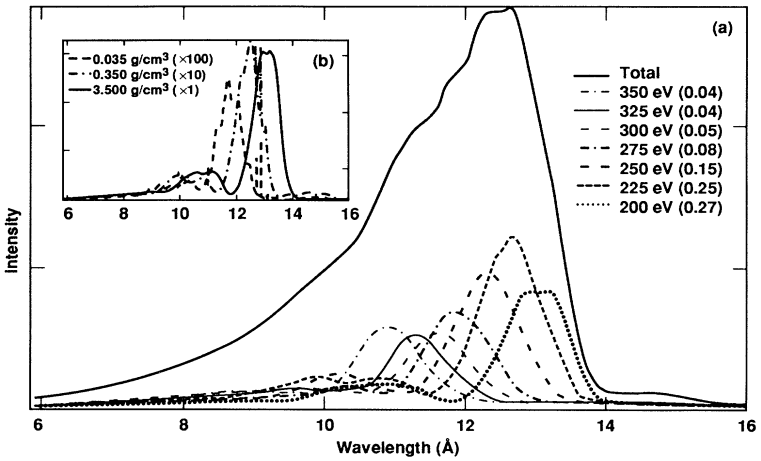

FIG. 4. (a) STA model for the spectrum in Fig. 1. Solid trace is the sum of the spectra obtained for each temperature, weighted by the fractions in parentheses. (b) Density dependence of STA $n=3-4$ peak position at 200 eV. (The intensities for 0.35 and 0.035 g/cm^3 have been scaled by factors of 10 and 100, respectively, relative to the normal density trace.)

well represented assuming a distribution of temperatures between 200 and 350 eV, and that the peak emission corresponds to a temperature around 225 eV. (Discrepancies between the measured and model spectra are attributable to emission from lower densities—between solid and coronal—and higher and lower temperatures than those shown.)

Note that the position of the peak emission, corresponding in this case to $n=3-4$ transitions, is a strong function of temperature. In Fig. 4(b), the peak is shown to vary with density as well, shifting to shorter wavelength with decreasing density. Since the model assumes LTE, this trend is easy to understand: three-body recombination is suppressed at lower densities, leading to a more highly ionized charge-state distribution and, thus, more energetic bound-bound transitions. The model, then, strongly suggests that LTE emission from lower density regions does not contribute appreciably, since these regions are almost certainly at *higher* temperature than the normal density plasma.

Based on general features of the measured spectrum and the fit obtained in the STA model, we conclude that emission in the 9–15-Å band is dominated by radiation from a normal density plasma at a temperature between 200 and 300 eV. The data is consistent with this plasma being in LTE, and optically thin. Emission from lower-density, higher-temperature regions is not apparent, and is not required to explain the observations.

A cool, dense emitting plasma is formed early in time by skin-depth absorption and a thermal wave propagating into the solid material. If the region does not ablate during the laser pulse, but remains at high density, it will rapidly recombine once the drive is off, effectively localizing the emission in space and time. If, on the other hand, the plasma ablates before it recombines through the M shell, the drop in density will "freeze" a charge-state distribution reflecting LTE at low temperature and high density, and emission will be nonlocal, persisting into the corona. Such coronal emission ought to contribute structure on top of the high-density background. Since the spectral measurement integrates over all time, even weak emission, if persistent, could easily swamp the early-time component. Although there are hints of this structure in the data, it clearly does not suggest appreciable late-time or coronal emission.

We must also consider the possibility that, though emission comes from a high-density plasma localized early in time, there is insufficient time for the charge-state distribution to equilibrate. Our LTE model is hardly applicable in this case, and the temperature inferred thereby will be incorrect. It is difficult to dispose of this possibility without supplementing the spectral evidence with a simulation of the experiment. But we can, at least, check the consistency of the LTE hypothesis by comparing collisional ionization times with the ~1-ps pump duration. Assuming $T_e \sim 250$ eV and solid density, and using the Lotz formula [15], the total LTE ionization rate for an $n=3$ electron of nickel-like barium is $\sim 6\times 10^{-11}$ cm^3 sec^{-1}, indicating that electron densities of only $\sim 2\times 10^{22}$ cm^{-3}, well below that of the solid, are needed at this temperature.

Our assumptions and conclusions are substantiated by simple hydrodynamic simulations. We simulated the experiment in one dimension, with an incident laser flux of 5×10^{15} W/cm^2 and 30% absorption, using the Lagrangian hydrodynamic code LASNEX [16], with hydrogenic, non-LTE average-atom atomic physics (XSN) [17]. Laser energy was deposited by both inverse bremsstrahlung and resonant absorption at the critical surface, $N_c = 1.6\times 10^{22}$ cm^{-3}. We found that assuming 30% absorption at N_c best reproduced the observed position of the Ba emission maximum at about 12.5 Å. Resonant absorption is restricted to the ablated corona, where suprathermal electron temperatures of several keV, and fractions as high as 95% are generated [18]. The thermal electron temperatures, however, do not exceed 350 eV, as shown in Fig. 5(a), and peak just after the peak of the laser pulse at 1 ps. Note that peak temperatures are reached later for deeper zones, owing to thermal transport. Figure 5(b) shows that the electron density rises initially in each zone, as the plasma is heated and stripped, then drops as the material expands.

In Fig. 6, we plot integrated radiant energy output as a function of time in the band from 900 to 1100 eV. Evidently, over 80% of the emission into this band takes place in the first 4 ps following onset of the pump; at the

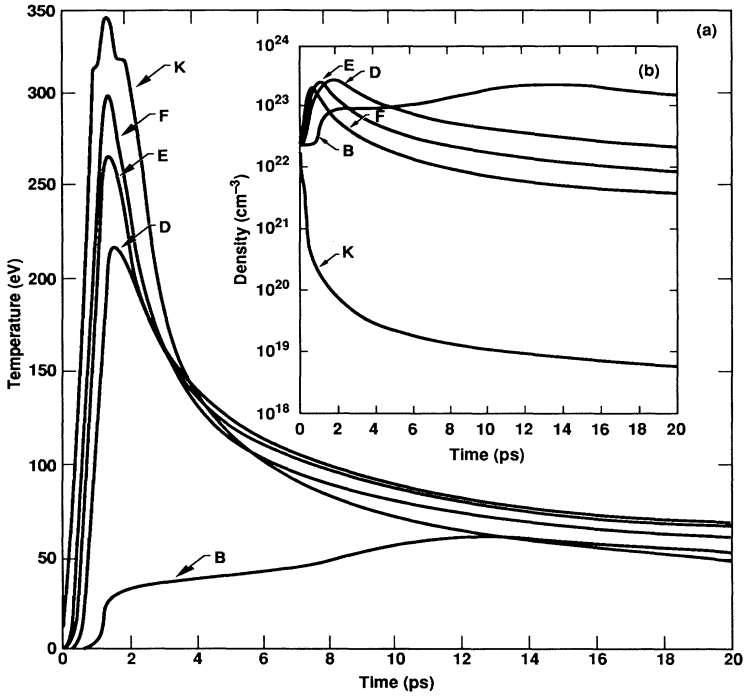

FIG. 5. As predicted by LASNEX, (a) the thermal electron temperature and (b) electron density, as functions of time, in a series of Lagrangian zones: *K* is the front surface of the 2 μm target; *F*, *E*, and *D* are, respectively, 0.02, 0.05, and 0.12 μm deep initially, and *B* is at 0.7 μm. These zones are chosen to represent three regions: the blow-off plasma (*K*); the emitting plasma (*F*,*E*,*D*) at $\sim$100–1000 Å, heated by thermal transport; and a deeper region, > 1000 Å, that does not participate in the emission or ablation.

emission peak, $\sim$1000 eV, the figure is over 90%. Localization of the emission in this band in both space and time is further demonstrated in Fig. 7. Finally, at the time of peak emission (2 ps), in zones *D*, *E*, and *F*, LASNEX predicts mean occupancies of the *M* shell of 17.8, 16.9, and 16.2 electrons, respectively. The corresponding LTE values, also calculated by LASNEX, are 17.6, 17.3, and 16.4.

In conclusion, we have observed x rays in the 9–15-Å band emitted from a solid target of BaF_2 irradiated by $\sim$100 mJ of 0.25 μm, KrF, light in a 650-fs FWHM Gaussian laser pulse. We have successfully modeled the observed spectrum using the STA theory and concluded that the emitting region is at comparatively low temperature (200–300 eV) and high electron density (10^{23}–10^{24} cm^{-3}), and is localized in both space and time. This in-

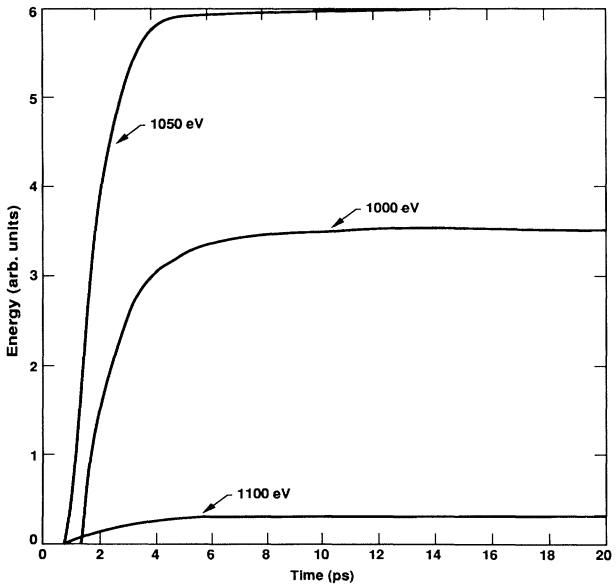

FIG. 6. Radiated energy (arbitrary units) as a function of time at 1000, 1050, and 1100 eV. The global emission peak is between 1000 and 1050 eV.

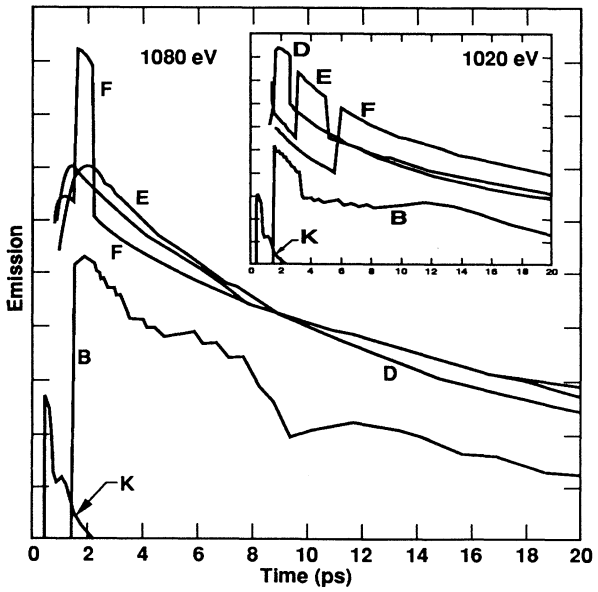

FIG. 7. Emission in arbitrary logarithmic units at 1080 eV and, inset, at 1020 eV, as a function of time in zones *K*, *F*, *E*, *D*, and *B*. The emission is highly localized in space and time. Emitting zones have temperatures of 200–300 eV, and electron densities of $\sim 3\times10^{23}$ cm^{-3}. The inset abscissa also covers the time range from 0 to 20 ps.

terpretation is reinforced by LASNEX simulations that indicate that emission in this band closely tracks the laser pulse. We expect to be able to apply an understanding of this localization to develop spectroscopic diagnostics for ultrashort-pulse laser-produced plasmas.

The authors thank Dr. M. Rosen for valuable assistance in simulating the experiment and Dr. A. Osterheld for providing atomic data. Work performed under the auspices of the U.S. Dept. of Energy by the Lawrence Livermore National Laboratory under Contract No. W-7405-Eng-48, the U.S. Air Force Office of Scientific Research under Grant No. AFOSR 89-0159, the Department of Energy under Grant No. DE-F602091ER12108, the U.S. Office of Naval Research and the Strategic Defense Initiative Organization.

[1] N. H. Burnett and P. B. Corkum, J. Opt. Soc. Am. B **6**, 1195 (1989); M. M. Murname, H. C. Kapteyn, and R. W. Falcone, IEEE J. Quantum Electron. **25**, 2417 (1989); C. J. Keane, J. N. Bardsley, L. da Silva, N. Landen, and D. Matthews, in *Femtosecond to Nanosecond High Intensity Lasers and Applications,* edited by E. M. Campbell, Proc. SPIE Vol. 1229 (SPIE, Bellingham, WA, 1990), pp. 190–195.

[2] M. M. Murname, H. C. Kapteyn, and R. W. Falcone, Phys. Rev. Lett. **62**, 155 (1989); M. M. Murname, H. C. Kapteyn, M. D. Rosen, and R. W. Falcone, Science **251**, 531 (1991).

[3] R. Fedosejevs, R. Ottmann, R. Sigel, G. Kühnle, S. Szatmari, and F. P. Schäfer, Phys. Rev. Lett. **64**, 1250 (1990); R. M. More, Opt. Soc. Am. Tech. Dig. Ser. **17**, 67 (1989); H. M. Milchberg, R. R. Freeman, S. C. Davey, and R. M. More, Phys. Rev. Lett. **61**, 2364 (1988).

[4] J. A. Cobble, G. A. Kyrala, A. A. Hauer, A. J. Taylor, C. C. Gomez, N. D. Delameter, and G. T. Schappert, Phys. Rev. A **39**, 454 (1989).

[5] A. Zigler, P. G. Burkhalter, D. J. Nagel, K. Boyer, T. S. Luk, A. McPherson, J. C. Solem, and C. K. Rhodes, Appl. Phys. Lett. **59**, 777 (1991).

[6] A. Zigler, P. G. Burkhalter, D. J. Nagel, M. D. Rosen, K. Boyer, G. Gibson, T. S. Luk, A. McPherson, and C. K. Rhodes, Appl. Phys. Lett. **59**, 534 (1991); A. Zigler, P. G. Burkhalter, D. J. Nagel, J. C. Solem, K. Boyer, T. S. Luk, A. McPherson, D. A. Tate, and C. K. Rhodes (unpublished).

[7] C. H. Nam, W. Tighe, S. Suckewer, J. F. Seely, U. Feldman, and L. A. Woltz, Phys. Rev. Lett. **59**, 2427 (1987).

[8] C. H. Nam, W. Tighe, E. Valco, and S. Suckewer, Appl. Phys. B **50**, 275 (1990).

[9] A. Zigler, P. G. Burkhalter, D. J. Nagel, M. D. Rosen, K. Boyer, T. S. Luk, and C. K. Rhodes, Opt. Lett. **16**, 1261 (1991).

[10] A. Bar-Shalom, J. Oreg, W. H. Goldstein, D. Shvarts, and A. Zigler, Phys. Rev. A **40**, 3183 (1989).

[11] T. S. Luk, A. McPherson, K. Boyer, and C. K. Rhodes, Opt. Lett. **14**, 1113 (1989).

[12] J. Bauche, C. Bauche-Arnoult, and M. Klapisch, Adv. At. Mol. Phys. **23**, 131 (1988).

[13] G. Mehlman, P. G. Burkhalter, D. A. Newman, and B. H. Ripin, J. Quant. Spectrosc. Radiat. Transfer **45**, 225 (1991).

[14] R. D. Cowan, *The Theory of Atomic Structure* (University of California, Berkeley, 1981).

[15] W. Lotz, Astrophys. J. Suppl. Ser. **14**, 207 (1967).

[16] G. B. Zimmerman and W. L. Kruer, Comments Plasma Phys. Controlled Fusion **11**, 51 (1975).

[17] W. A. Lokke and W. H. Grassberger, Lawrence Livermore National Laboratory Report No. UCRL-52276, 1977 (unpublished).

[18] D. W. Forslund, J. M. Kindel, and K. Lee, Phys. Rev. Lett. **39**, 284 (1977).